

Department of Mechanical Engineering and Mechanics

Drexel University College of Engineering

The following item is made available as a courtesy to scholars by the author(s) and Drexel University Library and may contain materials and content, including computer code and tags, artwork, text, graphics, images, and illustrations (Material) which may be protected by copyright law. Unless otherwise noted, the Material is made available for non profit and educational purposes, such as research, teaching and private study. For these limited purposes, you may reproduce (print, download or make copies) the Material without prior permission. All copies must include any copyright notice originally included with the Material. **You must seek permission from the authors or copyright owners for all uses that are not allowed by fair use and other provisions of the U.S. Copyright Law.** The responsibility for making an independent legal assessment and securing any necessary permission rests with persons desiring to reproduce or use the Material.

Please direct questions to archives@drexel.edu

Drexel University Libraries
www.library.drexel.edu



<http://www.drexel.edu/>

Precision extruding deposition and characterization of cellular poly- ϵ -caprolactone tissue scaffolds

F. Wang, L. Shor, A. Darling, S. Khalil, W. Sun, S. Güçeri and A. Lau

The authors

F. Wang, L. Shor, A. Darling, S. Khalil, W. Sun, S. Güçeri and A. Lau are all based at the Department of Mechanical Engineering and Mechanics, Drexel University, Philadelphia, USA.

Keywords

Advanced manufacturing technologies, Scaffolds, Biological analysis and testing

Abstract

Successes in scaffold guided tissue engineering require scaffolds to have specific macroscopic geometries and internal architectures to provide the needed biological and biophysical functions. Freeform fabrication provides an effective process tool to manufacture many advanced scaffolds with designed properties. This paper reports our recent study on using a novel precision extruding deposition (PED) process technique to directly fabricate cellular poly- ϵ -caprolactone (PCL) scaffolds. Scaffolds with a controlled pore size of 250 μm and designed structural orientations were fabricated.

Electronic access

The Emerald Research Register for this journal is available at
www.emeraldinsight.com/researchregister

The current issue and full text archive of this journal is available at
www.emeraldinsight.com/1355-2546.htm

1. Introduction

Three-dimensional (3D) scaffolds play important roles in scaffold guided tissue engineering because they provide critical functions as extracellular matrices onto which cells can attach, grow, and form new tissues. Design and fabrication of tissue scaffolds is always a challenged subject in regenerative medicine, particularly for load bearing scaffolds in bone and cartilage tissue engineering application. To design this type of tissue scaffold often needs to address multiple biological, mechanical and geometrical design constraint in terms of scaffold external and internal geometry, porosity, pore size and interconnectivity in order to provide the needed structural integrity, strength, transport property, and an ideal micro-environment for cell and tissue ingrowth and healing (Hollister *et al.*, 2002; Hutmacher, 2000; Sun and Lal, 2002). Advances in computer-aided tissue engineering and the use of biomimetic design approach enable to introduce biological and biophysical requirement into the scaffold design (Sun *et al.*, 2003 a, b). However, thus designed scaffolds often have intricate architectures that can only be fabricated through advanced manufacturing techniques. Most available scaffold fabrication methods, such as solvent casting, fiber bonding, phase separation, gas induced foaming, and salt leaching, are either limited to produce scaffolds with simple geometry, or to depend on in-direct casting method for scaffold fabrication (Taboas *et al.*, 2003; Yang *et al.*, 2002), so they are impractical for being used to manufacture scaffolds with complex structural architectures. To overcome this hurdle, solid freeform fabrication techniques, such as 3D printing, multi-phase jet solidification, and fused deposition modeling (FDM) have been widely adopted for scaffold fabrication (Koch *et al.*, 1998; Wu *et al.*, 1996; Zein *et al.*, 2002). Among the reported

The authors acknowledge the NSF-0219176 project funding support to graduate students Andrew Darling and Saif Khalil, and the ONR research funding support to graduate student Lauren Shor. The authors also would like to thank Dr P. Lelkes at Drexel University for his advice and access to the Cellular Biological and Tissue Engineering Laboratory for the biological study.

techniques, FDM-based extruding deposition seems to be one of the most promising processes because of its versatility of using different scaffolding materials, possibility of manufacturing scaffolds in a cell-friendly environment, and feasibility of controlled drop-on-demand high precision deposition (Vozzi *et al.*, 2002; Xiong *et al.*, 2001).

On the other hand, the ability of quantification of the scaffold fabrication-microstructure relationships, such as the effect of the process on the morphologies and the functional properties of the scaffolds, is as important as the scaffold fabrication itself because the biological and mechanical functions of the scaffold are in part dominated by the fabricated local micro-architecture of the scaffold. Micro-computed tomographic (micro-CT) imaging technology enables the characterization of the salient features of the scaffolds for tissue engineering applications. Recent reports have shown that micro-CT techniques are capable of characterizing micro-architectural and mechanical properties of tissue scaffolds (Lin *et al.*, 2003), evaluating porous biomaterials (Müller *et al.*, 1996), quantifying the bone tissue morphologies and internal stress-strain behavior (Van *et al.*, 1999) and conducting nondestructive evaluation for tissue properties (Müller and Rügsegger, 1997).

The objective of this paper is to present our recent study on using a precision extruding deposition (PED) process to fabricate poly- ϵ -caprolactone (PCL) tissue scaffolds with designed micro-architecture, and to present the study on using micro-CT technique for evaluation and characterization of the morphologies and microstructures of the PED fabricated scaffolds. In contrast to the conventional FDM process that requires the use of precursor filaments, the presented PED process directly extrudes scaffolding materials in its granulated or pellet form without the filament preparation and freeform deposits according to the designed microscale features. A brief outline of the fabrication procedure, including the description of the PED system major components, the PED process and the scaffold architecture, and the use of the PED process to freeform fabricate cellular PCL scaffolds is introduced in Section 2. Section 3

presents the material and the process. Section 4 reports a summary of the study on using SEM, micro-CT and the experimental testing to characterize the morphology, internal geometry, mechanical property and biological compatibility of the as-fabricated scaffolds, followed by a conclusion and discussion in Section 5.

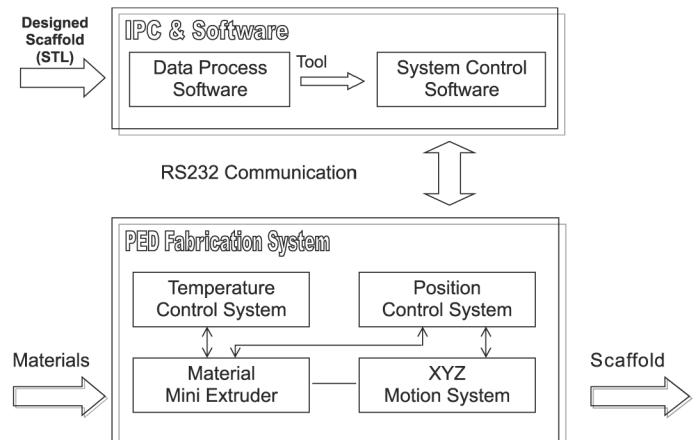
2. System configuration for PED

2.1 PED system

A PED system developed at Drexel University (Bellini, 2002) was used for this study. A schematic configuration of the PED system is shown in Figure 1. The hardware component consists of an XYZ position system, a material extruder system, and a temperature control system. The software component consists of a data processing software and a system control software. The data processing software slices the STL files and generates the process toolpath. The system control software controls the material deposition according to the process toolpath to form a layered 3D object.

The material mini-extruder system delivers the PCL in a fused form through the deposition nozzle. The major difference of the PED process with the conventional FDM process lies in that the scaffolding material can be directly deposited through PED process without involving filament preparation. The pellet-formed PCL is fused by a liquefier temperature provided by two heating bands and respective

Figure 1 Configuration of the PED fabrication system



thermal couples and then extruded by a pressure created by a turning precision screw. A schematic of the material mini-extruder system is shown in Figure 2.

To achieve deposition accuracy, the positioning system and the material mini-extruder are synchronized as shown in Figure 3. The material deposition roads (of both contouring and raster filing) consist of series of line segments, so the extruder movement is composed of a series of 2D linear interpolations upon which a simultaneous proportional signal to the XY position is extracted. The signal is used to drive the rotating motor of the material extruder. The proportional ratio can be adjusted to coordinate the positioning system and material dispensing system according to its controlled movement, speed, and material extrusion flow rate.

Figure 4 shows the information pipeline during the fabrication process. The designed scaffold CAD model is first converted into STL format, and then sliced with each slice patterned stored in the pattern library for toolpath generation. Initialized by a parameters file, the in-house developed system control software provides functions for 3D part visualization, machine and process setup, testing and

monitoring during the real-time fabrication process.

3. Materials and process

PCL (Sigma Aldrich Inc., Milwaukee, Wisconsin) in the form of pellets was used as the scaffolding material. PCL is a semi-crystalline aliphatic polymer that has a slower degradation rate than most biopolymers in its homopolymeric form. It has a low glass transition temperature at -60°C , a melting temperature at about $58\text{--}60^{\circ}\text{C}$, and a high thermal stability. It has a high decomposition temperature T_d of 350°C . The mechanical properties of PCL ($M_w = 44,000$) with a tensile strength of 16 MPa, tensile modulus of 400 MPa, flexural modulus of 500 MPa, elongation at yield of 7.0 percent, and elongation at break of 80 percent have been reported.

A designed scaffold cylinder model, measuring 20 mm in diameter and 10 mm in height, was first created in a CAD format. This cylinder CAD model was converted to a STL format then sliced into layers. Each layer was then filled with the designed scaffold pattern to generate toolpath file. The strands of PCL were extruded in four distinct layer patterns: 0, 90, 60, and 120° (designated P1, P2, P3 and P4, respectively), or alternating layers of $60^{\circ}/120^{\circ}$ with different gap lengths between the strands. The definition of scaffold layout pattern is shown in Figure 5.

4. Evaluation of morphology, mechanical and biological properties

4.1 Results of scaffold fabrication

A set of PCL scaffolds was fabricated using the PED system. The following processing parameters were used for all scaffold fabrication: the processing liquefier temperature 90°C , the orifice diameter of the tip 0.25 mm, and deposition velocity at 20 mm/s. The filling gaps of 0.42 and 0.51 mm were applied for two different sets of scaffolds. For each scaffold, there are a total of 39 layers with each layer thickness at 0.254 mm. The scaffold patterns were either $0^{\circ}/90^{\circ}$ (three samples), or $0^{\circ}/120^{\circ}$ (three samples), or combined $0^{\circ}/120^{\circ}$

Figure 2 Schematic of material mini-extruder

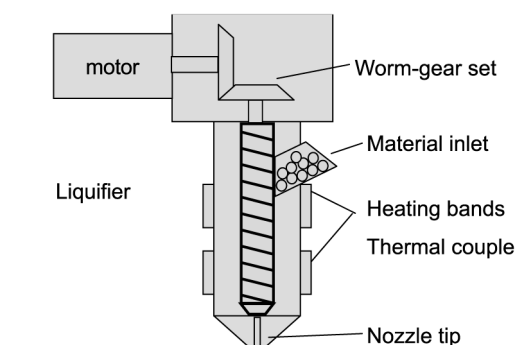


Figure 3 Synchronization of positioning and material dispensing system

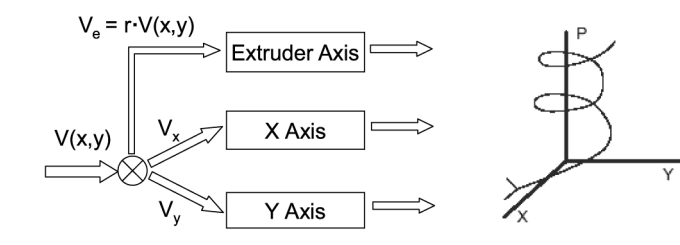
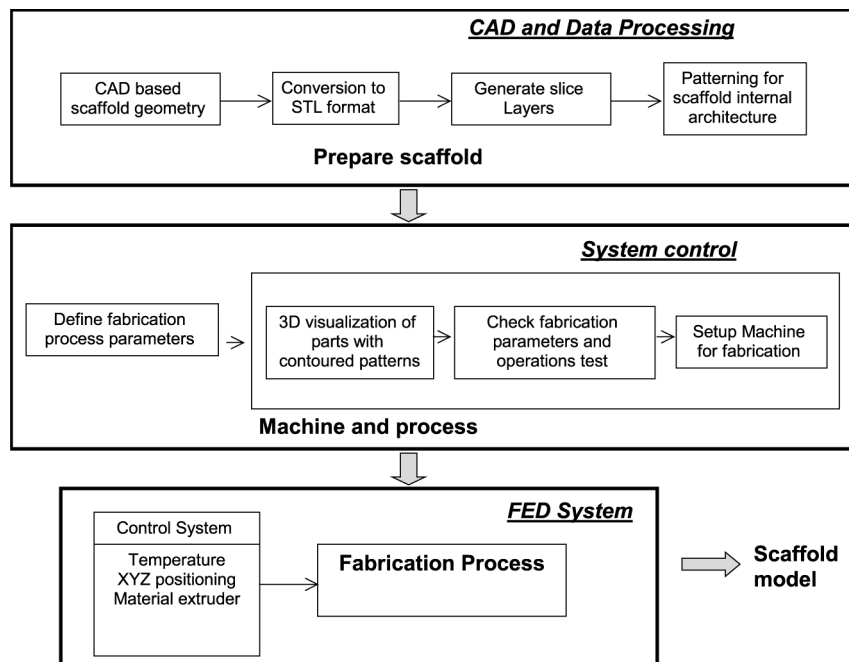
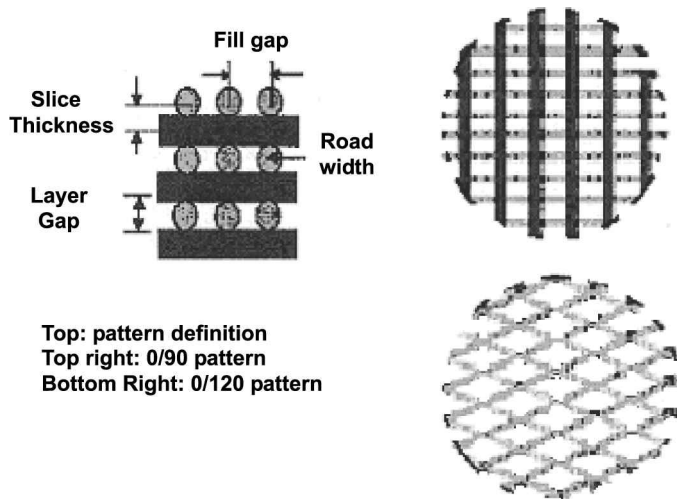


Figure 4 Information process of the manufacturing system**Figure 5** Definition of scaffold layout pattern

(for top 19 layers) and 0°/90° (for bottom 20 layers) pattern.

4.2 Evaluation of morphology, mechanical and biological properties

The effect of the PED process on the morphology and structure of the as-fabricated scaffolds were evaluated using SEM and micro-CT. The compression tests were also conducted to evaluate the mechanical strength of the as-fabricated scaffold. Preliminary biological experiments were also conducted to evaluate the

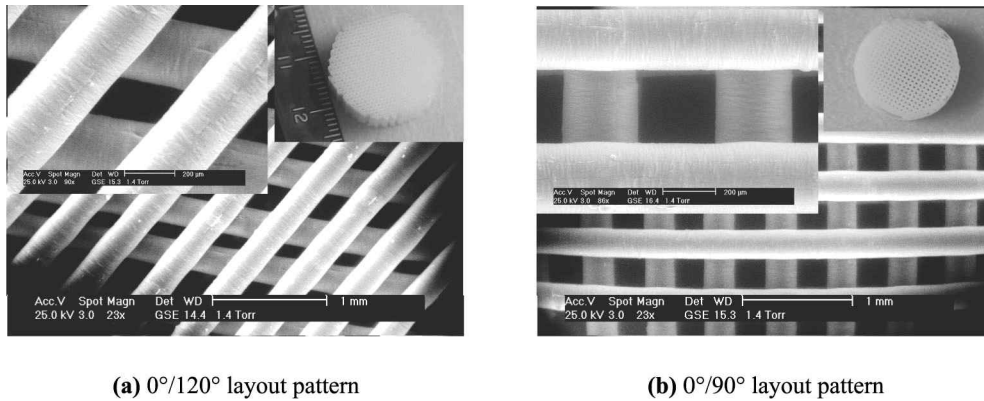
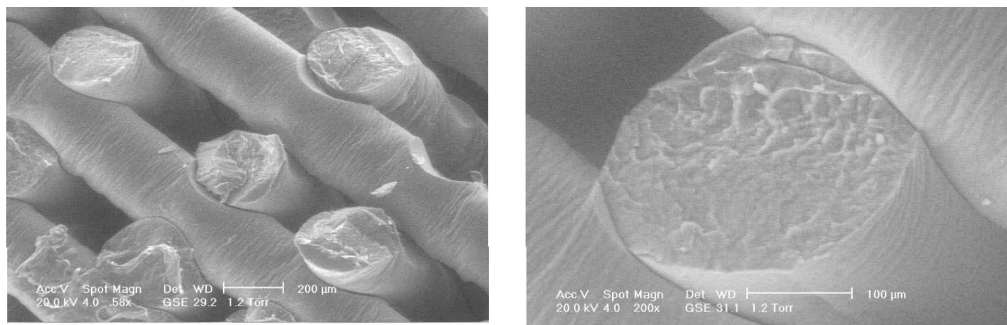
biocompatibility of the scaffold. Descriptions of the evaluations, results and experimental procedures are presented as follows.

4.2.1 SEM imaging characterization

FEI/Phillips XL-30 field emission environmental scanning electron microscope (ESEM) was used to evaluate the micro-structural formability and internal morphologies of as-fabricated scaffolds. The SEM images were taken using a beam intensity at 20.0 keV and the gaseous secondary electron detectors at 1.3 Torr. The SEM images of scaffolds are shown in Figure 6(a) (for 0°/90° deposition pattern) and Figure 6(b) (for 0°/120° deposition pattern), along with the images of the as-fabricated scaffolds. Both SEM images clearly present that the fabricated micro-architecture of the scaffolds could be achieved at about 250 μm scale level. The good uniformity of the fill gaps and the depositing struts shown in Figure 6, and the internal pore connectivity shown in Figure 7 demonstrate the applicability of using the PED process to fabricate PCL scaffolds at micro-scale level.

4.2.2 Micro-CT imaging based 3D morphological characterization

Micro-CT enables 3D characterization of the salient features, the structural formability

Figure 6 SEM image scaffold with different layout pattern**Figure 7** SEM image (section view) of internal pore connectivity

and the morphologies of the as-fabricated PCL scaffolds. The micro-CT was set at 19.1 μm resolution. 2D analyses and 3D reconstructions of core regions of the sample scaffolds were performed. These results illustrate that qualitative and quantitative analysis of polymer scaffolds is possible through micro-CT and 3D reconstruction techniques.

Micro-CT imaging acquisition. SkyScan 1072 micro-CT desktop scanner (Skyscan, Belgium) was used to scan the internal architecture of the scaffold. The output format for each sample was approximately 500 serial 1,024 \times 1,024 bitmap images. These slice images were analyzed in SkyScan's Tview software. Initially, length measurements were taken around the sample to determine the degree to which the sample conformed to the cylindrical template. Volume analyses were performed on the center of each sample. Volume fraction and surface per unit volume were determined in 3D analysis, and relative area was measured in ten randomly selected slice images in 2D analysis. Ten strut

and pore widths were measured in 2D images from each sample.

3D reconstruction. 3D reconstruction was performed using Mimics software (Materialise, Belgium) with pre-processing using ImageJ. Sixty-two sequential 200 \times 200 pixel images were cropped from the serial images from the center of each sample. Imported into Mimics, these serial core images were reconstructed into 3D volumetric models. Thresholds were inverted to allow measurement of the volume of all pore spaces within the model. Subsequently, a region-growing operation was performed, creating a mask consisting only of interconnected pore spaces. Volume for this region-grown mask was determined and the ratio of region-grown volume to the total volume was calculated. The percentage of this ratio is defined as the degree of interconnectivity.

A summary of data retrieved from the analysis through Tview is displayed in Table I. The results also include the measurements of individual strut and pore widths based on the

Table I Summary of the micro-CT morphological analyses

Sample	SP-1	SP-2	SP-3	SP-4
Max./Min. diameter (mm)	19.74/18.79	19.62/18.59	19.44/18.51	19.56/18.57
Surface (mm ²)	9,219	20,854	18,936	10,036
Relative area (percent)	60.89	55.8	47.28	44.24
Total volume (mm ³)	490	1,004	957	458
Volume fraction (percent)	60.8	53.1	47.4	45.1
Strut width ($n = 10$, mm)	0.264 ± 0.023	0.264 ± 0.023	0.270 ± 0.019	0.250 ± 0.034
Pore width ($n = 10$, mm)	0.196 ± 0.054	0.210 ± 0.089	0.254 ± 0.034	0.292 ± 0.04

2D serial slice imaging. Ten measurements were taken for each sample in this analysis. 3D reconstructed models by using Mimics are displayed in Table I with a sample of corresponding 2D images and the characterized porosity and interconnectivity of each sample. Results of micro-CT imaging based 3D reconstruction, porosity and interconnectivity analyses are shown in Figure 8.

4.2.3 Compression experiment

The Instron 5800R machine was used for the test of as-fabricated scaffold. The initial strain rate of the tests was adjusted to 10 percent per minute at the beginning of the test and no preload was applied before initiating compression testing. Standard solid compression platens were used for testing. Stress-strain data were computed from load-displacement measurements. Compressive modulus was determined based on the slope of the stress-strain curve in the elastic region. The data were corrected on the strain axis to a value of approximately 0.025 for calculating the

compressive elastic modulus of the scaffold. The stiffness of the machine was also put into the calculations to decrease machine error.

Three SP-2 specimens were tested under compression to a limit of specific compressive displacements. The PCL specimens were measured for their dimensions for accurate area calculations. The scaffolds were cylindrically shaped with minute irregularities on the circumference wall due to specimen processing. The samples were tested at a speed of 0.1 mm/min at a room temperature of 24°C with a relative humidity of 15 percent. The average data of the test results are plotted in Figure 9.

4.2.4 Preliminary biological experiments

Preliminary biological experiments have been conducted to study the basic scaffold biocompatibility. These experiments were intended to address the issue of free radicals caused by heating of the polymer and whether these radicals would be detrimental to cell growth. Another question was whether the pore size of approximately 250 μm would be

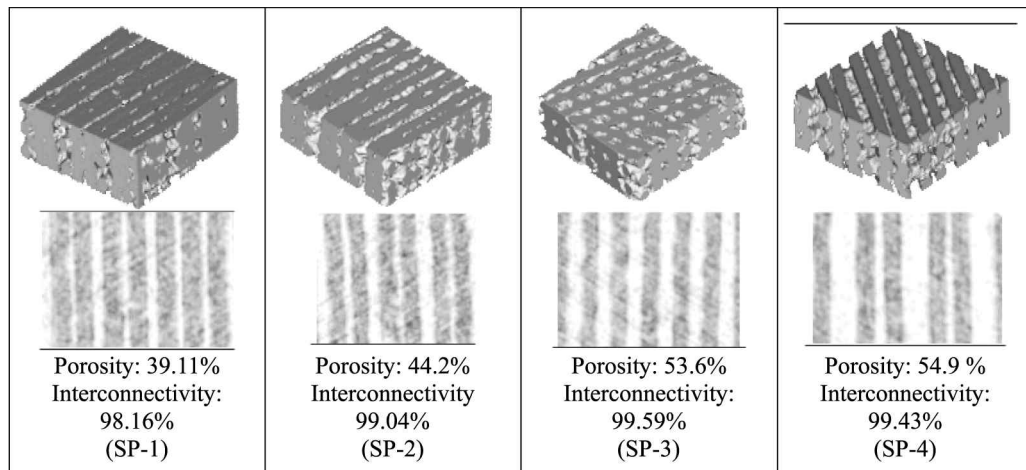
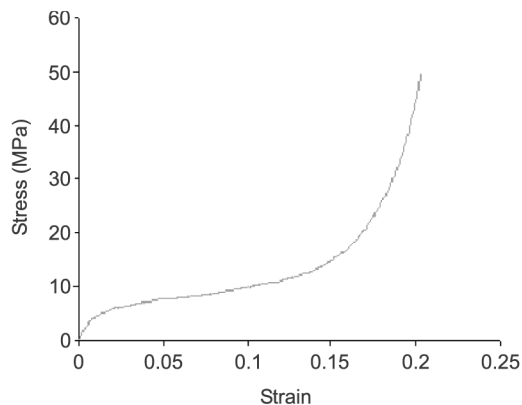
Figure 8 Micro-CT imaging based 3D reconstruction, porosity and interconnectivity analyses

Figure 9 PED as-fabricated scaffold stress-strain curve under compression test



conductive to cell growth alone or would require a filler material.

Cardiomyoblasts (H9C2) were seeded onto three sets of 90° scaffolds, one set with no filler material, one with collagen filling the pores, and one with fibrin gel filling the pores. Initial seeding size was approximately 10^5 . All samples showed cell attachment to the scaffold on the fifth day, and a monolayer of cells atop the scaffold sample. Displayed in Figure 10 are (from left to right), a scaffold without filler material, a scaffold with fibrin gel filler, and a close-up of a single fibrin filled pore. The confluence of the monolayer atop the scaffold on the fifth day indicates uninterrupted cell growth. We feel that this illustrates a proof of concept and the PCL scaffold post-heating is not immediately detrimental to seeded cells.

The presence of a material greatly enhanced proliferation and differentiation of cells, as indicated by the visible cellular processes in the figure. This would indicate that a 250 μm pore size may be too large enough to optimally enhance cardiomyoblast growth. While 250 μm is ideally suited for the free diffusion of oxygen, the cells were unable to cross the pore spaces

without the presence of a fibrin gel filler material. Currently, quantitative proliferation and attachment studies are being performed for three cell types with cytofluorimetry, fluorescence microscopy, and immunofluorescence as methods of analysis.

For the comparative proliferation study, 10^4 cardiomyoblasts, fibroblasts, and smooth muscle cells were seeded upon 90° PCL scaffolds of 1 mm thickness without filler material. Cell numbers were measured using Alamar blue staining and cytofluorimetry. Initial results showed that anchorage-dependent cells such as fibroblasts are better able to take advantage of the scaffold microarchitecture without a filler material. The fibroblasts attach to the surfaces preferentially compared to polystyrene and progressively grow into the porespace, narrowing the channel. Qualitatively, the ingrowth of the fibroblasts is such that it may close off pores completely. While the sample scaffolds for this proliferation study were thin (1 mm), the fibroblast ingrowth may reduce nutrient flow in thicker scaffolds. Followup studies are underway focusing on fibroblasts, examining long-term growth, the occurrence of pore closure, and the effects of scaffold thickness on proliferation.

5. Conclusions

A study on using PED process to freeform fabricate cellular PCL scaffolds and on using SEM, micro-CT and the experimental testing to characterize the morphology, internal geometry, mechanical property and biological compatibility of the as-fabricated scaffolds were conducted. Both hardware and software configuration of the PED process system were described and the PCL scaffolds with controlled internal architectures were produced. Results of

Figure 10 Results of preliminary biological experiments



the characterization demonstrated the capability of the PED fabrication process in manufacturing the PCL scaffolds with microstructure and pore size at about 250 μm scale. This process directly fabricates tissue scaffolds by converting designed architecture into layered deposition pattern without involving the material preparation and in-direct casting, and thus opens opportunities for complex scaffold fabrication.

Results of the characterization also show that micro-CT is a capable tool for nondestructive evaluation of PCL scaffolds. The use of 2D analysis and 3D reconstruction software allows the examination of morphologies, internal architecture, the interconnectivity of as-fabricated tissue scaffolds, and provides a quantitative measurement of porosity and micro-architecture. As shown in the analysis, a typical pore size of the fabricated scaffold range from 200 to 300 μm , near the optimal size suggested for bone tissue scaffold application. In addition, strut width is consistent between samples, all samples showed greater than 98 percent interconnectivity. The scaffold compression modulus obtained from the test is in the range between 150 and 200 MPa. The preliminary result of biological experiments demonstrated the biocompatibility of the process and material, and also suggested larger spaces for further investigation and improvement. All these suggest the viability of the fabrication and the characterization process, as well as its potential applications in tissue engineering.

References

- Bellini, A. (2002) "Fused deposition of ceramics: a comprehensive experimental, analytical and computational study of material behavior, fabrication process and equipment design", PhD dissertation, Department of Mechanical Engineering and Mechanics, Drexel University.
- Hollister, S.J., Maddox, R.D. and Taboas, J.M. (2002), "Optimal design and fabrication of scaffolds to mimic tissue properties and satisfy biological constraints", *Biomaterials*, Vol. 23, pp. 4095-103.
- Hutmacher, D.W. (2000), "Scaffolds in tissue engineering bone and cartilage", *Biomaterials*, Vol. 21, pp. 2529-43.
- Koch, K.U., Biesinger, B., Arnholz, C. and Jansson, V. (1998), "Creating of bio-compatible, high stress resistant and resorbable implants using multiphase jet solidification technology", *Rapid News Publication*, pp. 209-14.
- Lin, A.S.P., Barrows, T.H., Cartmell, S.H. and Guldberg, R.E. (2003), "Micro-architectural and mechanical characterization of oriented porous polymer scaffolds", *Biomaterials*, Vol. 24, pp. 481-9.
- Müller, R. and Rügsegger, P. (1997), "Micro-tomographic imaging for the nondestructive evaluation of trabecular bone architecture", in Lowet, G. et al. (Eds), *Bone Research in Biomechanics*, IOS Press, Amsterdam, pp. 61-80.
- Müller, R., Matter, S., Neuenschwander, P., Suter, U.W. and Rügsegger, P. (1996), "3D Micro tomographic imaging and quantitative morphometry for the nondestructive evaluation of porous biomaterials", in Briber, R., Pfeiffer, D.G. and Han, C.C. (Eds), *Morphological Control in Multiphase Polymer Mixtures*, *Mat. Res. Soc. Proc.*, 461, pp. 217-22.
- Sun, W. and Lal, P. (2002), "Recent development on computer aided tissue engineering – a review", *Computer Methods and Programs in Biomedicine*, Vol. 67, pp. 85-103.
- Sun, W., Darling, A., Starly, B. and Nam, J. (2004a), "Computer aided tissue engineering: part I – overview, scope and challenges", *Journal of Biotechnology and Applied Chemistry*, Vol. 34.
- Sun, W., Starly, B., Darling, A. and Gomez, C. (2004b), "Computer aided tissue engineering: part II – application in biomimetic modeling and design of tissue scaffold", *Journal of Biotechnology and Applied Chemistry*, Vol. 34, in preparation.
- Taboas, J.M., Maddox, R.D., Krebsbach, P.H. and Hollister, S.J. (2003), "Indirect solid free form fabrication of local and global porous, biomimetic and composite 3D polymer-ceramic scaffolds", *Biomaterials*, Vol. 24, pp. 181-94.
- Van R., Müller, R., Ulrich, D., Rügsegger, P. and Huiskes, R. (1999), "Tissue stresses and strain in trabeculae of canine proximal femur can be quantified from computer reconstructions", *J. Biomech.*, Vol. 32, pp. 165-74.
- Vozzi, G., Previti, A., Rossi, D. and Ahluwalia, A. (2002), "Microsyringe-based deposition of two-dimensional and three-dimensional polymer scaffolds with a well-defined geometry for application to tissue engineering", *Tissue Engineering*, Vol. 8, pp. 1089-98.
- Wu, B.M., Borland, S.W., Giordano, R.A., Cima, L.G., Sachs, E.M. and Cima, M.J. (1996), "Solid free-form fabrication of drug delivery devices", *Journal of Controlled Release*, Vol. 40, pp. 77-87.
- Xiong, Z., Yan, Y., Zhang, R. and Sun, L. (2001), "Fabrication of porous poly(L-lactic acid) scaffolds for bone tissue engineering via precise extrusion", *Scripta Materialia*, Vol. 45, pp. 773-9.
- Yang, S., Leong, K., Du, Z. and Chua, C. (2002), "The design of scaffolds for use in tissue engineering. Part 2. Rapid prototyping techniques", *Tissue Engineering*, Vol. 8 No. 1, pp. 1-11.
- Zein, I.W., Hutmacher, D.W., Tan, K.C. and Toch, S.H. (2002), "Fused deposition modeling of novel scaffold architecture for tissue engineering application", *Biomaterials*, Vol. 23, pp. 1169-85.